

ON THE STABILIZATION OF RETAINED AUSTENITE

F.B. Abudaia

Department of Materials and Metallurgical Engineering,
Al-Fateh University B.O. Box 13430, Tripoli, Libya
E-mail: fabudaia@yahoo.com

المخلص

عادة ما تحتوي الطبقات المصلدة في الصلب على نسب صغيرة من طور الأوستنيت المتبقي (غير المتحول). إحدى الطرق المتبعة لتخفيض محتوى طور الأوستنيت في مثل هذه الحالات هو استخدام التبريد العميق عن طريق الغمر في النيتروجين السائل. سيتم في هذا البحث تقييم زيادة ثبات طور الأوستنيت مع التقادم بمدى صعوبة تحول طور الأوستنيت المتبقي إلى طور المارتنيت باستخدام عمليات الغمر بعد وقبل التعتيق. في هذا البحث تمت دراسة تأثير التقادم على ثبات طور الأوستنيت مع استبعاد تأثير الإجهادات المتخلفة الناتجة من جسم المشغولات الكربنة وذلك باستخدام عينات من الصلب الكربوني بسمك 1 مم لمحاكاة الطبقة المصلدة في عمليات الكربنة. تم استخدام حيود الأشعة السينية لحساب نسب طور الأوستنيت المتبقي وللكشف عن التغيير في المحتوى الكربوني في طوري الأوستنيت و المارتنيت وحساب الإجهادات الداخلية الناتجة عن تحول طور الأوستنيت إلى المارتنيت بالطبقة المصلدة .

بمقارنة النتائج (مخططات حيود الأشعة السينية) لعدة عينات تم إخضاعها لعمليات تعتيق وغمر مع أخرى غير معتقة وجد إن عمليات التعتيق تؤدي إلى زيادة ثبات طور الأوستنيت مع التقادم وأن نشؤ إجهادات ضغط متخلفة صغيرة بداخل الطبقة المصلدة نتيجة تحول طور الأوستنيت إلى المارتنيت قد يؤدي إلى منع تحول إضافي من طور الأوستنيت إلى المارتنيت. لوحظ عدم تغيير في المحتوى الكربوني لطور الأوستنيت بسبب عمليات التعتيق وأن المحتوى المرتفع لعنصر الكربون بطور الأوستنيت المتبقي يصاحب هذا الطور قبل عملية التعتيق.

يرجح أن يكون السبب الرئيسي لزيادة ثبات طور الأوستنيت المتبقي أثناء التعتيق هو إعادة توزع الكربون عن طريق نزوح الكربون من طور المارتنيت أثناء التعتيق كما هو واضح من اختفاء الازدواج في قيم طور المارتنيت في مخططات حيود الأشعة وانتشاره إلى الخلاعات في الحدود الفاصلة بين طوري الأوستنيت و المارتنيت مما يؤدي إلى إعاقة حركة الحدود الفاصلة وبالتالي زيادة صعوبة تحول طور الأوستنيت المتبقي إلى طور المارتنيت أثناء عمليات التبريد اللاحق بالغمر .

ABSTRACT

Carburized layers in quenched steel components usually contain few percent of retained austenite (RA). Deep freezing treatment by dipping in liquid nitrogen is usually carried out when it is required to reduce the amount of retained austenite to very low levels. Stability of retained austenite due to aging was assessed by the difficulty of transformation of retained austenite to martensite when subjected to sub-zero treatment. In this work the case material was simulated by carburizing thin specimens of 1mm thick to obtain full through hardening by carburization. Retained austenite was found to

stabilize with aging. Even in the absence of the effect of the core material, the retained austenite become under small compressive stresses induced by previously transformed austenite. This state of stress opposes further transformation resulting in incomplete transformation of austenite to martensite. X-Ray Diffraction (XRD) patterns from aged and non-aged specimens do not reveal any austenite carbon enrichment with aging. Indication of carbon atoms redistribution during aging is observed by disappearance of peak doublets of martensite lines on XRD diffraction patterns. Impeding mobility of $\bar{\alpha}/\gamma$ interface by migration of carbon atoms to dislocation arrays is more likely to occur. Stability of retained austenite could therefore be attributed to the lowered mobility of the $\bar{\alpha}/\gamma$ interface.

KEYWORDS: Retained austenite; Deep freezing; Carburization; X-ray diffraction pattern; Aging

INTRODUCTION

The microstructure produced in quenched-case carburized alloy steels consists of martensite with some RA. The amount of retained austenite usually present in the microstructure affects mechanical properties [1,2] and dimensional stability [3]. Apart from the discussion concerning the beneficial or deleterious effects of retained austenite on hardened steel parts, controlling the amount of retained austenite should always be important. In engineering applications where dimensional tolerance is very important any delayed transformation of retained austenite to martensite during service will affect the accuracy of components dimensions. Residual stresses generated during service due to austenite transformation could cause premature failures in tooling components [4].

Carburization is an effective process to increase surface hardness and induce compressive stresses at surface layers to improve fatigue and wear resistance. During cooling the carburized layer tries to expand to accommodate the increase in volume resulted from the austenite to martensite transformation. Compressive stresses are set up when core material imposes constraint on the expanding surface layers. As the austenite to martensite transformation is accompanied by increase in volume, applied or residual compressive stresses will resist transformation. Therefore compressive stresses generated in the carburized layer during quenching in conjunction with the higher carbon content in the last remaining austenite will prevent complete transformation. In this work it is aimed to examine whether carbon enrichment during aging is the responsible mechanism for stability of retained austenite. In order to eliminate the effect of compressive stresses induced by the core material, specimens tested were made of comparable thickness of the case depth of about 1 mm thick to simulate the case material. Thus thin specimens are through hardened during the carburization process.

MATERIALS AND METHODOLOGY

Increase of carbon content of the austenite phase can be detected using X-ray diffraction. Brag's law correlates the diffraction angle to the interplanar distance (d spacing) as follows:

$$\lambda = 2d_{hkl} \sin \theta \quad (1)$$

where λ is the x-ray wavelength, d_{hkl} is the interplanar spacing of $\{hkl\}$ planes and θ is the diffraction angle. Interplanar spacing for a given plane is related to the lattice parameter (a_o) through the plane miller indices.

$$d_{hkl} = \frac{a_o}{\sqrt{h^2 + k^2 + l^2}} \quad (2)$$

where a_o is the lattice parameter.

The lattice parameter (a_o) of a given lattice varies with the presence of alloying elements. The effect depends on the type and amount of the foreign atoms. For instance, the lattice parameter of the austenite phase in steel varies with the carbon content according to the following equation. [5].

$$a_o = 3.555 + .044 \times \text{wt\%C} \quad (3)$$

where wt%C is the carbon content in wt%. Effects of substitutional alloying elements such as Si and Mn are minor on the lattice parameter [6, 7].

The lattice parameter of the austenite phase can be determined from the peak position (2θ) on the X-ray diffraction pattern. Interplanar spacing also varies with either applied stress or residual stresses. Tensile stresses will increase the spacing and compressive stresses will decrease it. The change in peak position ($\Delta 2\theta$) is directly related to the stress level as given by the following equation [5].

$$\sigma_\phi = k_1(\Delta 2\theta) \quad (4)$$

where σ_ϕ is the induced stress in MPa and k_1 is the stress constant ($= 595 \text{ MPa} / \Delta 2\theta$) for steel.

Different heat treatment schemes include different combinations of quenching and aging were applied. X-ray diffraction patterns were obtained for the various heat treatments schemes. Variations of carbon content during aging or induced stresses due to transformation were detected separately.

Peak positions (2θ values) and peak intensities corresponding to martensite and retained austenite phases were determined from X-ray diffraction patterns. Percentages of retained austenite were calculated using the direct comparison method [8] which depends on the relative peak intensities of both phases. Peak positions (2θ values) determine the interplanar spacings which are affected by the carbon content and state of stress. Therefore any carbon enrichment due to aging in the austenite phase can be detected.

The nominal composition of test specimens is given in Table 1. This steel (SAE grade 832M13) is a case hardenable grade and it was selected because of its Nickel content which promotes stability of the austenite phase.

Table 1: Nominal chemical composition of the as received material in wt%

Composition							
C	Si	Mn	P	S	Cr	Mo	Ni
0.10-0.16	0.10-0.35	0.35-0.60	0.035	0.065	0.70-1.0	0.10-0.25	3.00-3.75

Specimens with dimensions of 20 mm x 20 mm x 1 mm were prepared for the carburization process. Figure 1 shows a photograph of a test specimen. Pack carburization was carried out at 950°C for 7 hrs. The carburization mixture contains 3% BaCO₃ and 3% CaCO₃ added to charcoal. These conditions should produce through hardening in specimens resembling carburized layers in case hardened steels. The scheme of work is explained in the flow chart shown in Figure 2. All specimens were carburized under the same conditions of temperature and time then subjected to different treatments as indicated by schemes A, B, C and D in Figure 2.

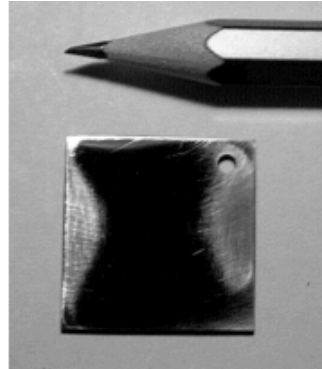


Figure 1: Test specimen

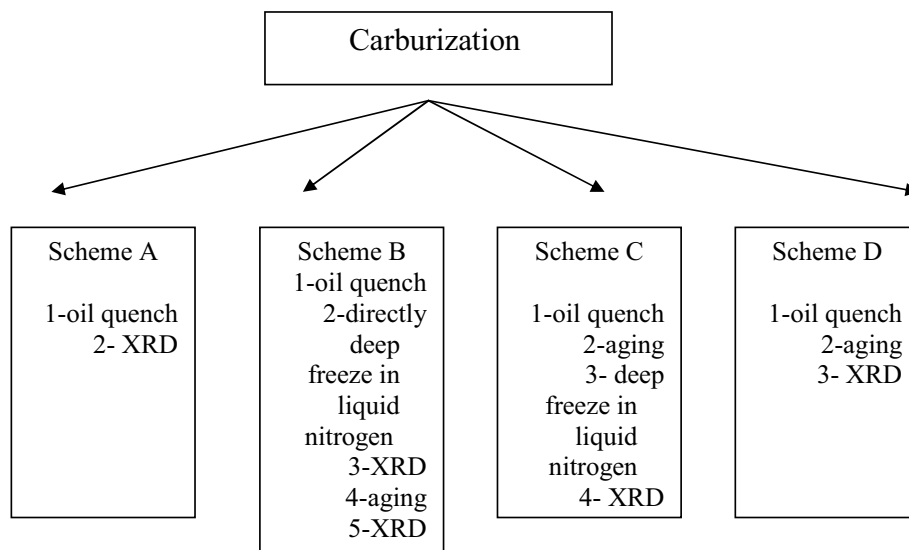


Figure 2: Schemes of various heat treatments

In scheme B two XRD patterns were obtained, one is immediately after deep freezing and another XRD diffraction pattern was obtained after the specimen had been aged for 30 days. Aging was carried out at room temperature. Specimen surfaces were then pickled chemically and carefully ground to avoid strain transformation of retained austenite. Patterns of X-ray diffraction were obtained using X-Ray diffractometer type 9XS Bruker D 5005 with Cu $k_{\alpha 1}$ radiation with wavelength of 1.5406 Å.

The relative amount of retained austenite produced with various heat treatments schemes are estimated according to the direct comparison method using the following equation [5]:

$$\frac{I_{\gamma}}{I_{\alpha}} = \frac{R_{\gamma} C_{\gamma}}{R_{\alpha} C_{\alpha}} \quad (5)$$

where I is the integrated intensity of the diffraction line and

$$R = \left(\frac{1}{v^2} \right) \left[|F|^2 P \left(\frac{1 + \cos^2 2\theta}{\sin^2 \theta \cos \theta} \right) \right] (e^{-2M}) \quad (6)$$

v is the volume of unit cell, F is the structure factor, P is the multiplicity factor, θ is the Bragg angle and e^{-2M} is the temperature factor.

The relative amounts of martensite C_{α} and austenite C_{γ} are obtained using the relationship:

$$C_{\alpha} + C_{\gamma} = 1 \quad (7)$$

RESULTS AND DISCUSSION

X-ray Diffraction patterns obtained with various heat treatment schemes are shown in Figures 3 to 7. Diffraction patterns show that all hardened specimens consist of martensite and retained austenite. These two phases are readily identified in XRD diffraction patterns. Martensite is characterized by diffraction peaks from planes $\bar{\alpha}_{200}$, $\bar{\alpha}_{211}$ and $\bar{\alpha}_{220}$ while the austenite phase by peaks from γ_{200} , γ_{220} and γ_{311} . The strongest diffraction peaks of $\bar{\alpha}_{110}$ and γ_{111} are very close and these lines are avoided in any calculation. Variation in peaks positions and shapes in various schemes reflects changes that take place due to carbon content or induced stresses. Accurate calculations and data were obtained from enlarged XRD patterns.

Effect of aging on stability of retained austenite.

To assess the increased stability of retained austenite with time, XRD patterns from schemes A, B and C were compared. Austenite diffraction peaks from γ_{200} and γ_{220} was compared with martensite diffraction peaks from $\bar{\alpha}_{200}$ and $\bar{\alpha}_{211}$ in the three patterns. The calculated relative amounts of retained austenite using the direct comparison method from these three specimens are shown in Table 2. Substantial amount of retained austenite is produced in carburized specimens due to the high carbon content and the presence of nickel.

The oil quenched specimen (scheme A) showed the highest amount of retained austenite (20.5 %). The retained austenite content is reduced to 11.2 % after direct deep freezing. When oil quenched specimens are aged for 30 days before deep freezing, the amount of retained austenite is reduced only to 16 %. This comparison show that retained austenite resists transformation to martensite and becomes more stable with aging treatment.

Table 2: Relative amounts of retained austenite in specimens A, B and C

Heat treatment scheme	% of retained austenite
A	20.5
B	11.2
C	16

Effect of internal stress

Carburized specimens used in this work are 1 mm thick to resemble the carburized layer in the hardened steel components. In carburization heat treatment, the high level of compressive residual stresses induced in the carburized layer is due to the constraint imposed by the core material on the carburized layer. Therefore when thin specimens are through hardened the effect from the core material is eliminated. Any stresses generated in the carburized specimens should be attributed to phase transformation and not due to constraint.

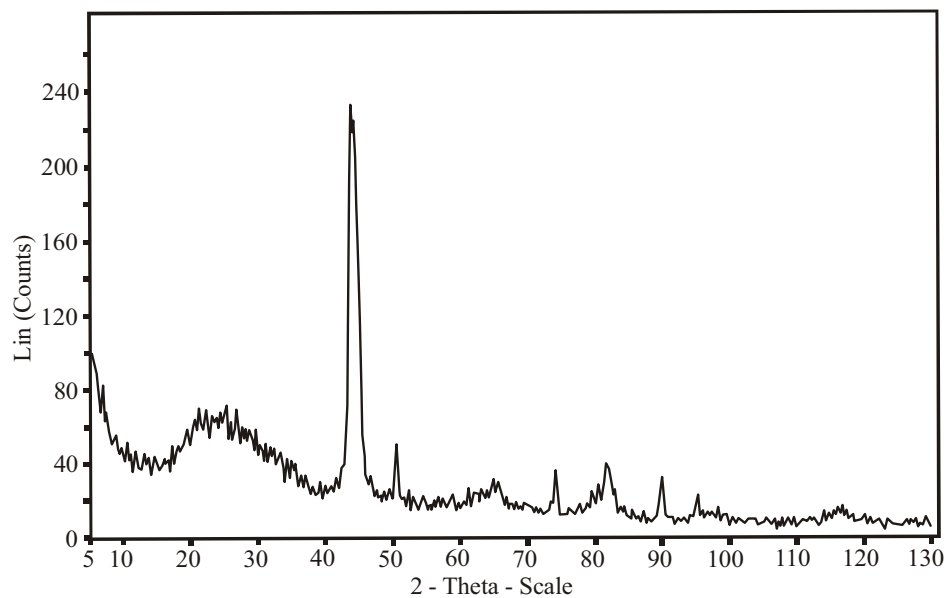


Figure 3: XRD pattern of oil quenched-specimen treated according to scheme A.

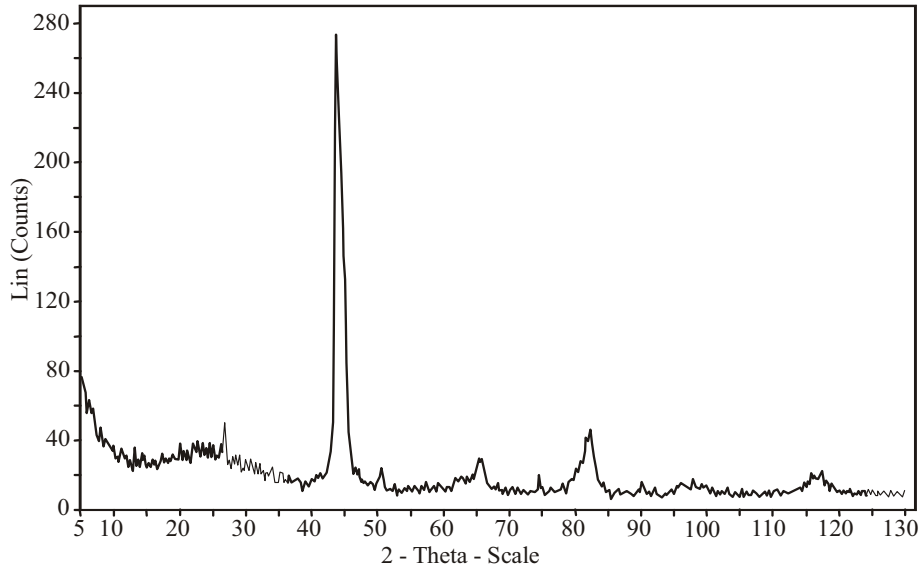


Figure 4: XRD pattern directly after deep freezing of specimen treated according to scheme B

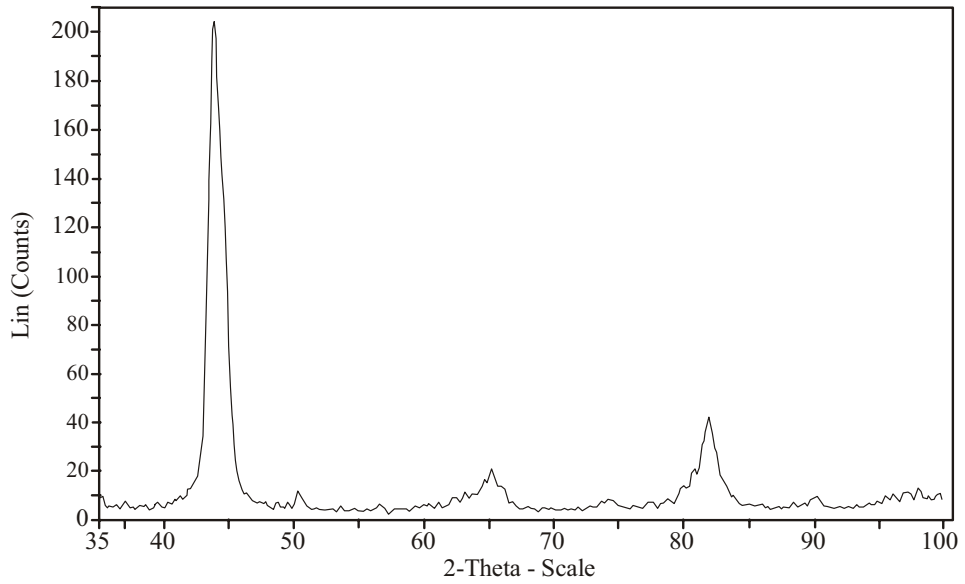


Figure 5: XRD pattern after deep freezing following by 30 days of aging- specimen treated according to scheme B.

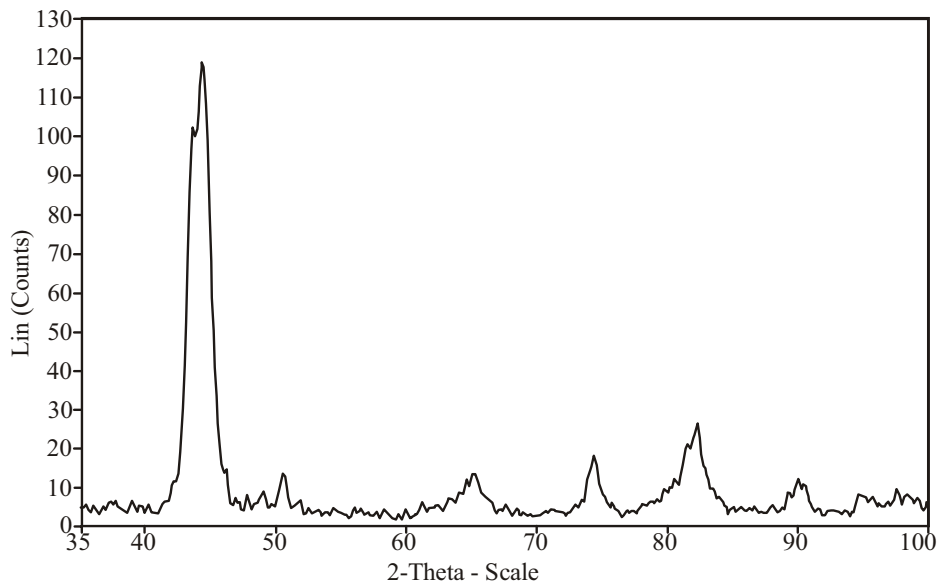


Figure 6: XRD pattern after oil quenching- aging and then deep freezing- specimen treated according to scheme C.

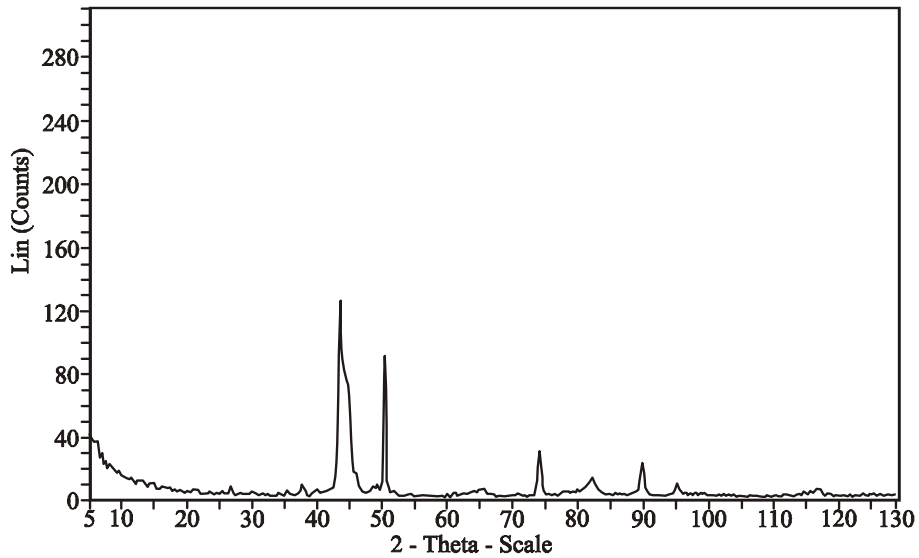


Figure 7: XRD pattern after oil quenching and aging for 30 days -specimen treated according to scheme D

Comparison of patterns from schemes A and B revealed that the peak positions of the austenite phase are not identical. The peak position 2θ values of the austenite phase of

lines γ_{200} , γ_{220} and γ_{311} obtained from specimens treated in schemes A and B are shown in Table 3.

Table 3: Peak position 2θ values of the austenite phase in specimens A and B

Diffraction line	2θ values	
	Scheme A	Scheme B
γ_{200}	50.5	50.6
γ_{220}	74.2	74.5
γ_{311}	90.0	90.25

The deep freezing treatment for specimen treated by scheme B was carried out without any delay after oil quenching so that no time is available for any carbon atoms to migrate between phases. Therefore the change in 2θ values is attributed to the induced stresses and not to change in carbon content of the austenite phase. Table 3 shows that 2θ values have increased after deep freezing treatment. This is due to the increased amount of transformation of retained austenite to martensite and the compressive stress accompanied the transformation reaction. Therefore more compressive stresses will act on the retained austenite resulting in smaller interplanar distance of the austenite phase and larger 2θ values. The origin of this stress is the 4% increase in volume accompanying the austenite to martensite transformation. The induced compressive stresses will render the austenite more resistant to transformation. Retained austenite peaks in XRD patterns corresponding to lines 200, 220 and 311 from schemes A and B (Figures 3 and 4) also showed that peaks had broadened in specimen subjected to deep freezing. Peak broadening is due to either strained structure or finer grained structure. This means that as transformation of austenite to martensite proceeds, retained austenite is subjected to higher compressive stresses and transformation becomes more difficult.

The level of the induced stresses due to deep freezing treatment corresponding to such change in 2θ can be estimated using equation (4)

$$\sigma_{\phi} = k_1(\Delta 2\theta) \quad (4)$$

The estimated induced stress is about 1 to 3 MPa. This is a small stress comparing with compressive stresses normally obtained in carburization treatments for thicker components. This confirms that compressive stresses are mainly generated because of the constraint effect imposed on the surface layers by the core material and the gradient of carbon content.

Carbon redistribution

Carbon redistribution during aging was examined by comparing XRD patterns of oil quenched and deep frozen specimens without aging and after aging. XRD pattern of Figure 3 obtained immediately after oil quenching (without aging) is compared with pattern of Figure 7 obtained after aging for 30 days. For deep frozen specimens, patterns of Figures 4 and 5 obtained from freshly deep frozen specimen and after aging for 30 days respectively were also compared. No obvious variations in 2θ values of the austenite lines with aging for both sets could be noticed. These comparisons do not

reveal evidence of carbon enrichment of the austenite phase during aging. However comparisons of these patterns showed that peaks doublets due to martensite lines $\bar{\alpha}_{200}$ and $\bar{\alpha}_{211}$ become more pointed and the doublets nearly disappeared after aging but no change in 2θ values are observed. Peak doublets of martensite lines are due to the tetragonality of the martensite unit cell. Disappearance of doublets could be due to decreased tetragonality of martensite caused by carbon diffusion out of the tetragonal cells of the martensite phase. This means that carbon redistribution occurs during aging.

It has been proposed by Sarikaya *et al* [9] that carbon enrichment in retained austenite phase is possible resulting in a higher carbon content of the retained austenite than the overall carbon content. They also found higher carbon concentration at the $\bar{\alpha}/\gamma$ interface, but the average carbon content in the austenite phase was higher than the nominal content in the investigated steels. They did not observe partitioning of substitutional elements such as Cr, Ni, Mn and Si. Wang and Van Der Zwaag [10] concluded that chemical stabilization due to the enrichment of carbon in the retained austenite is the most important mechanism for the austenite retention.

The higher carbon content of retained austenite could be inherited from the initial austenite phase before quenching. Transformation to martensite starts at grains of less carbon content as its M_s temperature is higher. As the temperature decreases during quenching, areas of higher carbon content progressively transform. At the same time as the reaction proceeds the remaining austenite is affected upon by ever increasing compressive stresses resulting from previously transformed grains. Thus grains with the highest carbon content are more likely to remain untransformed. The carbon content of the austenite phase of the current treated specimens was estimated using equations 1-3. Taking the 2θ values as indicated in Table 2 for the specimen treated according to scheme A and the wavelength of $\text{Cu } k_{\alpha 1}$ radiation as 1.5406 Å, the carbon content of the retained austenite was found about 1.3 wt %. The austenite carbon content is therefore higher than the average carbon content in the specimens. Table 4 shows the spectrometer chemical analysis obtained after carburization for a representative test specimen. The carbon content increased during carburizing from about 0.1 wt % to about 1.0 wt %. The carbon content in the retained austenite is about 30 % higher than the average carbon content. This higher content is thought to be inherited from initial austenite as explained earlier.

Table 4: Chemical composition of carburized specimen (wt%)

Composition							
C	Si	Mn	P	S	Cr	Mo	Ni
1.064	0.32	0.43	0.01	0.02	0.69	0.098	2.97

Therefore it is more likely that stabilization of retained austenite during aging is not attributed to austenite enrichment with carbon. The stabilization mechanism could be attributed to redistribution of carbon atoms and diffusion of carbon atoms from the martensite phase to dislocations at the austenite-martensite interface which rendering the movement of the interface more difficult.

CONCLUSIONS

The stability of retained austenite due to aging in carburized specimens was studied. Sub-zero treatment by dipping in liquid nitrogen was applied to reduce the amount of retained austenite. It is found that retained austenite becomes more resistant to transformation with aging at room temperature. The effect of high compressive stresses imposed by the core material was eliminated by carburizing of thin specimens. Compressive stresses induced by previously transformed austenite are small and may not significantly affect the stability of the retained austenite. The higher carbon content of the retained austenite is not attributed to carbon enrichment of the austenite phase during aging but is inherited from the initial austenite. Carbon redistribution occurs during aging by diffusing out of the martensite phase. Therefore stability is caused by the retarded movement of the austenite-martensite interface by interstitial carbon atoms.

ACKNOWLEDGEMENTS

The author wishes to thank Eng. Yosef Soliman of the Industrial research center who carried out X-ray runs and also Engineers Naser Fadl and Moftah al-Zorgani of the advanced center of technology for heat treatment work.

REFERENCES

- [1] Kern R.F., Metals Progress, vol.166, no.1, July, 1972.
- [2] Magner S.H., Weins W.N. and Makinsons J.D., 19th Heat Treating Society Proceedings, Oct.1999.
- [3] Krauss G., Adv. Matl. & Proc. HTP, Sept.1995.
- [4] Wilson B.M. and Weins W.N., 2000, 20th ASM Heat Treating Society Conference Proceedings, 9-12 October 2000, St. Louis, MO, ASM International.
- [5] Cullity B.D., Elements of X-Ray diffraction, 2nd edition, Addison- Wesley, 1978.
- [6] Ruhl R.C. and Cohen M., Trans. AIME 245, 1969
- [7] Pearson W.B., A Handbook of Lattice Spacing and Structure of Metals and Alloys, Pergamon press, Oxford, 1958.
- [8] Averbach B.L. and Cohen M., Trans. AIME 176, 1948.
- [9] Sarikaya M., Thomas G., Steeds J.W., Barnard S.J. and Smith G.D.W., In proceeding of an International conference on solid-solid phase transformations August 10-14-1981, Metallurgical society of AIME 1982.
- [10] Wang J. and Van Der Zwaag S., Metallurgical and Materials Transaction A, vol.32A, June 2001